Eur. Phys. J. B **9**, 49–57 (1999)

THE EUROPEAN PHYSICAL JOURNAL B

EDP Sciences

Prediction of cell variations with pressure of ionic layered crystal Application to the matlockite family

F. Decremps[1,a], M. Fischer[1], A. Polian[1], J.P. Itié[1], and M. Sieskind[2]

[1] Physique des Milieux Condensés[b], Université Pierre et Marie Curie, B 77, 75252 Paris Cedex 05, France
[2] CNRS, laboratoire PHASE, B.P. 20, 67037 Strasbourg Cedex 2, France

Received 26 October 1998

Abstract. Compounds belonging to the matlockite family are ionic layered crystals. Some previous experimental studies on these compounds demonstrated the correlation between the difference in bond strength translating the layered properties and the anisotropic coordination of the highly polarizable halogen anion. In the present paper, we present a model to estimate the anisotropic compressibilities of matlockites which could be generalized to other ionic layered compounds. The compressibilities of each individual polyhedron which built the sheet of an ionic layered crystal are determined from a simple relation based on a semi-empirical relation obtained by Hazen *et al.*, involving the electrical charge of the ions and the interatomic distances. The electrical charge of the anions are taken to be direction-dependent and are modulated by the anion polarizability value. Finally, to validate the model, the calculated compressibilities are compared with previously published data, but also with new high pressure experimental data obtained by X-ray absorption spectroscopy up to 20 GPa on SrFCl and SrFBr at the K edge of the strontium and by X-ray diffraction up to 30 GPa on SrFBr and PbFBr. Present estimations give results which differ from the experimental values by less than 15%.

PACS. 64.30.+t Equations of state of specific substances – 62.20.-x Mechanical properties of solids – 61.10.Ht X-ray absorption spectroscopy: EXAFS, NEXAFS, XANES, etc.

1 Introduction

The experimental determination of the effect of pressure on the structural properties of layered ionic compounds has been extensively investigated in most cases because of their importance in geophysics, but also, more fundamentally, because the high pressure behaviour of these compounds gives an interesting insight on how the pressure affects weak and strong bonds in condensed matter. Unfortunately, the high sensitivity of lamellar compounds to deviatoric stresses or grain-grain contact effects, inherent to the high pressure techniques, creates undesirable effects which may overlap with the intrinsic structural behaviour.

It is therefore interesting to develop a simple method to estimate the linear and volumic compressibilities of ionic compounds characterized by an anisotropic bonding scheme. Hazen and Finger [1], following a study by Anderson and Nafe on the mineral compressibility [2], did propose a model to explain, reproduce, and predict the compressibility of three dimensional minerals. In the present work, we propose to adapt this model to bidimensional compounds in order to predict the structural behaviour of ionic layered crystals under high pressure.

To validate the model, a calculation of the compressibilities of matlockite-type compounds is undertaken and compared with the experimental results obtained by different techniques like ultrasonics [3–5] or X-ray diffraction [6,7]. To complete the previous published data on the matlockite compressibilities, X-ray absorption spectroscopy under high pressure has been carried out on two compounds of this family, SrFCl and SrFBr, which allowed to determine the local compressibility of the Sr-F bonds in both compound. The polyhedral method calculations are compared with these results in order to validate the Hazen semi-empirical relation which constitute the basis of this model. Finally, the equation of state of SrFBr and PbFBr have been determined by energy dispersive X-ray diffraction experiments under high pressure up to 30 GPa.

2 The MFX matlockites

The alkaline-earth fluorohalides MFX, where M = Ca, Sr, Ba, Pb or Eu and X = Cl, Br or I, form an important class of materials crystallizing in the PbFCl-type tetragonal structure $P4nmm$ (Fig. 1a), also called matlockite structure [8]. As illustrated in Figure 1b, the representation of the crystal structure as polyhedra simplifies the description of these compounds. The atomic arrangement

[a] e-mail: `fad@pmc.jussieu.fr`
[b] CNRS – UMR 7602

Table 1. Crystallographic data for selected matlockite type compounds. a and c are the lattice parameters in Å, u (halogen) and u' (metal) are coordinates, and d_{AB} is the distance between ions A and B.

	BaFCl[1]	BaFBr[1]	BaFI[1]	SrFCl[2]	SrFBr[3]	PbFCl[4]	PbFBr[5]	PbFI[5]
a (Å)	4.394	4.508	4.654	4.126	4.218	4.110	4.18	4.23
c (Å)	7.225	7.441	7.962	6.958	7.337	7.246	7.59	8.77
u	0.6472	0.6497	0.6522	0.6489	0.6479	0.6497	0.65	0.65
u'	0.2049	0.1911	0.1704	0.2015	0.1859	0.2058	0.195	0.167
dFF (Å)	3.106	3.187	3.290	2.917	2.982	2.906	3.18	3.36
dMF (Å)	2.649	2.665	2.693	2.494	2.511	2.539	2.56	2.58
dM′X (Å)	3.282	3.403	3.582	3.104	3.221	3.089	3.18	3.36
dM″X (Å)	3.194	3.409	3.844	3.110	3.387	3.216	3.45	4.30

in the matlockite structure is obtained by stacking successives sheets of MF_2 and MX_2: the MF_2 sublattice is formed by corner sharing cation-tetrahedra with a fluorine atom at the center (M_4F). The second sheet is made up of edge sharing cations pyramids (M_{4+1}-X). In these pyramids, the X halogen is on the four fold axis of the basal plane, at an height which is different in each compound. Hence, in general, the distance of X to the basal plane cations M′ is different from the distance to the M″ apex cation (Tab. 1) (therefore the notation M_{4+1}). Previous studies on several MFX compounds have shown that the anisotropic bonding scheme of these compounds depends, at ambient conditions, on the chemical nature of the M cations and, more drastically, of the X anions. For example, all the BaFX crystals are stabilized in the same P4nmm structure but with different layer character, as described by the following inequalities between the ratio B_c/B_a:

$$\left(\frac{B_c}{B_a}\right)_{\mathrm{BaFCl}} = 1.0 > \left(\frac{B_c}{B_a}\right)_{\mathrm{BaFBr}} = 0.8 > \left(\frac{B_c}{B_a}\right)_{\mathrm{BaFI}} = 0.45 \quad (1)$$

where $B_c(B_a)$ is the linear modulus along the $c(a)$ axis of the tetragonal MFX structure.

The cause of the observed anisotropy has been correlated [7,9] to the electronic polarizability α_X of the X anion (in Debye units, $\alpha_{Cl} = 2.96$, $\alpha_{Br} = 4.16$, $\alpha_I = 6.43$ [10]), which, and because of the asymmetric position of X inside the pyramid M_{4+1}-X, creates electrical dipole moments on the anion. For the most layered compounds (*e.g.* BaFI), the M′X bond is shorter than the M″X one (see Fig. 1b and Tab. 1), which imply a redistribution of the electrical charge density. The charges, accumulated in the four M′ cations plan, increase the linear modulus perpendicular to $C_4(B_a)$ by a simple steric effect. In parallel, the total charge on the iodine remaining constant, the electronic charge density of the M″X bond decreases, decreasing the linear modulus along $C_4(B_c)$. One the other hand, the chlorine in BaFCl is in a quasi-symmetric position inside the Ba pyramid, leading to a quasi-tridimensionnal structure ($B_c/B_a = 1$).

3 The Hazen polyhedral method

From the analysis of hundred minerals with different structures, Hazen *et al.* [1] proposed a simple model in order to predict and understand the volumic dependence of compounds submitted to an hydrostatic pressure. Briefly, the procedure consists at first to decompose the crystal into elementary polyhedra which generate the crystal unit-cell, and, secondly, to determine the individual compressibility χ(poly) of each polyhedron from a semi-empirical relation:

$$\chi(\mathrm{poly}) = A\frac{d^3}{Z_a Z_c} \quad (\mathrm{GPa}^{-1}) \quad (2)$$

where d, in Å, is the distance between an ion at the corner of the polyhedron and the ion inside the polyhedron. The constant A depends only on the chemical nature of the central ion (metal, halogen, ...) and $Z_{a(c)}$ is the mean anion (cation) valence.

Therefore, in this model, the compressibility of a polyhedron is isotropic. The polyhedra are considered as entities with a compressibility dependent only on the chemical nature of the ions and their mutual distances. Moreover, the previous considerations, and therefore the relation (2), are valid only for crystals where the repulsive interactions between the ions are limited to the first neighbours. In the opposite case, the model, based on the complete independence of the polyhedra, would not give good results.

Finally, the total crystal compressibility is deduced by summing the polyhedra properties by a procedure which depends on how the polyhedra are linked.

4 Polyhedra compressibilities of MFX matlockite compounds

In order to predict the matlockite polyhedra compressibilities, the following assumptions are made: a) anisotropic coordination of the halogen X inside the pyramid $M_{4+1}X$, b) dipole moment on X (large polarizability).

Hence, relation (2) may be rewritten as:

$$\chi_i(\mathrm{poly}) = \frac{1}{3}A\frac{d_i^3}{Z(\mathrm{M})Z_i(\mathrm{X})} \quad (\mathrm{GPa}^{-1}) \quad (3)$$

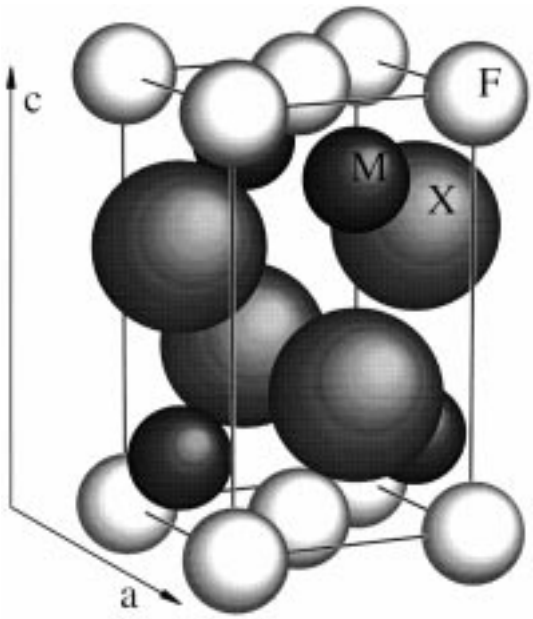

(a)

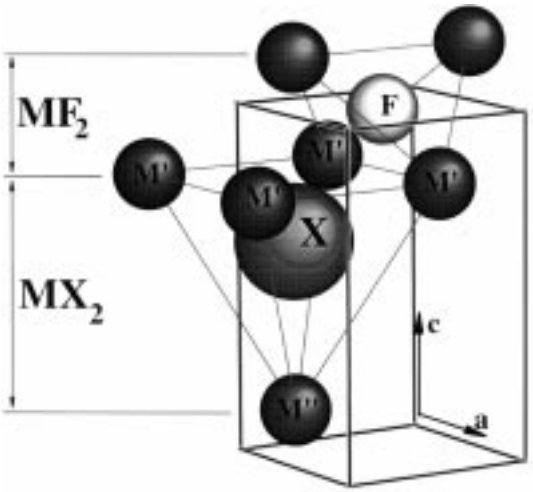

(b)

Fig. 1. (a) Example of the matlockite tetragonal structure MFX: BaFCl (a and c are the crystallographic axes). (b) Polyhedral representation of the matlockite structure. Contrary to the fluorine inside the M_4F tetrahedra, the halogen X is not equidistant from all the M cations which define the pyramid ($d_{M'X} \neq d_{M''X}$). (a and c are the crystallographic axes).

where χ_i(poly) is the polyhedron linear compressibility along the (i) direction (1/3 is related to the classical relation between volumic χ and linear compressibilities for isotropic compounds χ_i : $\chi_i = \chi/3$). d_i represents the anion-cation distance along the (i) direction, Z(M) the mean M cation valence and Z_i(X) the linear electrical charge of the anion X along the (i) direction, modulated in order to account for the halogen polarizability α_X.

For halogen ions, Hazen *et al.* determined a value of the constant A equal to 1.5×10^{-3} [1].

4.1 Compressibility of M_4F tetrahedra

For the complete set of studied compounds, the fluor is at the center of the tetrahedron, and hence equidistant to the metals M. Therefore, the classical model of Hazen is valid, giving the volumic compressibility χ(tetra):

$$\chi(\text{tetra}) = A\frac{d^3_{\text{MF}}}{Z(\text{M})Z(\text{F})} = 0.75 \times 10^{-3} d^3_{\text{MF}}. \qquad (4a)$$

Which leads to a linear relation:

$$\chi_i(\text{tetra}) = \frac{1}{3}A\frac{d^3_{\text{MF}}}{Z(\text{M})Z(\text{F})} = 0.25 \times 10^{-3} d^3_{\text{MF}} \qquad (4b)$$

with Z(M) = 2 and Z(F) = 1. The distances d_{MF} are reported in Table 1 and the results of the tetrahedra linear compressibilities in Table 2.

4.2 Compressibility of $M_{4+1}X$ pyramids

The halogen X, with a polarisability α_X, is in an asymmetric position inside the pyramid $M_{4+1}X$ so that two types of cation could be defined: $M_{4+1} = 4 \times M' + 1 \times M''$ (see Fig. 1b), with M″ at the top of the pyramid (the M″X bond is parallel to the C_4 axis), the four other cations M′ defining the base of the pyramid (a first approximation is to consider the M′X bond perpendicular to C_4). Moreover, the anisotropy observed in these crystal being clearly connected to the large polarizability of X [7,9], the $M_{4+1}X$ linear compressibilities perpendicular (parallel) to the C_4 axis $\chi_{\perp(\parallel)}$(pyr) can be simply characterized by three parameters $d_{M'X}$, $d_{M''X}$ and α_X:

$$\chi_\perp(\text{pyr}) = \frac{1}{3}A\frac{d^3_{m'X}}{Z(\text{M}')Z_\perp(\text{X})} \qquad (5)$$

$$\chi_\parallel(\text{pyr}) = \frac{1}{3}A\frac{d^3_{m''X}}{Z(\text{M}'')Z_\parallel(\text{X})} \qquad (6)$$

where $Z_\perp$(X) and $Z_\parallel$(X) represent respectively the perpendicular and parallel (to C_4) electronic charge of X. For all the matlockite compounds, X being an halogen (chlorine, bromine or iodine), the constant A is equal to 1.5×10^{-3}. The electronic charge on the cations is considered to be undistorded and $Z(\text{M}') = Z(\text{M}'') = 2$ will be taken.

The magnitude of Z_i(X) seen by the M cations depends on the distance between M and X, but also on the degree of polarizability of X. Moreover, it should be noted that:

(i) The total charge is constant:

$$Z_\perp(\text{X}) + Z_\parallel(\text{X}) = 2Z(\text{X}).$$

(ii) The electronic cloud is considered to be spherical when X is at the center of the pyramid:

$$Z_\perp(\text{X}) = Z_\parallel(\text{X}) = Z(\text{X}) \quad \text{if} \quad d_{M'X} = d_{M''X}.$$

Table 2. Polyhedra and crystal compressibilities χ (in 10^{-3} GPa^{-1}) for some PbFCl-type compounds deduced from the polyhedral method (calc.) and compared with experimental values (exp.). (a) and (b) refer respectively to the X-ray diffraction results (this work and [7]) and to the ultrasonics/Brillouin scattering values [4,5]. The interatomic distances in SrFI are not yet available and, as a consequence, no calculation was undertaken.

	BaFCl	BaFBr	BaFI	SrFCl	SrFBr	PbFCl	PbFBr	PbFI
R	1.028	0.997	0.932	0.997	0.950	0.960	0.922	0.781
B	0.0641	−0.0062	−0.133	−0.0069	−0.102	−0.087	−0.159	−0.437
$Z_\perp$	0.90772	1.00915	1.20098	1.01015	1.15209	1.12662	1.23694	1.65562
$Z_\parallel$	1.09228	0.99085	0.79902	0.98985	0.84791	0.87338	0.76306	0.34438
q_t	0.2577	0.2362	0.2054	0.2523	0.2283	0.259	0.242	0.200
q_p	0.7423	0.7638	0.7946	0.7477	0.7717	0.741	0.758	0.800
χ_i(tetra)	4.65	4.73	4.88	3.88	3.96	4.09	4.19	4.29
$\chi_\perp$(pyr)	9.72	9.74	9.55	7.37	7.24	6.54	6.50	5.73
$\chi_\parallel$(pyr)	7.43	10.00	17.72	7.60	11.49	9.52	13.45	57.7
$\chi_\perp$calc.	7.58	7.79	7.98	6.00	6.09	5.69	5.74	5.37
$\chi_\perp$exp.	7.5[a]	7.4[a]	6.6[a]	6.1[b]	5.6[a]	no data	6.0[a]	no data
$\chi_\parallel$calc.	6.71	8.76	15.08	6.66	9.77	8.16	11.21	47.00
$\chi_\parallel$exp.	7.3[a]	9.2[a]	14.3[a]	6.4[b]	8.6[a]	no data	11.2[a]	no data
$\chi_\perp/\chi_\parallel$calc.	1.13	0.89	0.53	0.90	0.62	0.70	0.51	0.11
$\chi_\perp/\chi_\parallel$exp.	1.0[a]	0.80[a]	0.45	0.95[b]	0.65[a]	–	0.50[a]	–
χcalc.	21.9	24.3	31.0	18.7	21.9	19.5	22.7	57.7
χexp.	22.2[a]	24.0[a]	28.0[a]	18.6[b]	19.8[a]	–	23.2[a]	–

As a consequence two simple relations between the linear and the volumic electronic charges are proposed:

$$Z_\perp(\mathrm{X}) = [2-(R+B)]Z(\mathrm{X}) \quad (7)$$

$$Z_\parallel(\mathrm{X}) = (R+B)Z(\mathrm{X}) \quad (8)$$

where R and B dimensionless parameters, introduced to account for the distorsion of the X electronic cloud:

– R defines the asymmetric position of the halogen:

$$R = d_{\mathrm{M'X}}/d_{\mathrm{M''X}} \quad (9)$$

– B quantifies the effect of the dipole moments:

$$B = \frac{\alpha_{\mathrm{X}}^{1/3}}{d_{\mathrm{MX}}}\left[\frac{d_{M'X}}{d_{M''X}} - 1\right]\cdot \quad (10)$$

The previous assumption is based on several arguments:

– The first factor at the right hand side of equation (10) ($\alpha_{\mathrm{X}}^{1/3}/d_{\mathrm{MX}}$), where d_{MX} corresponds to the mean value of the M-X distances, determines the average range of the halogen electrical dipoles effect. For a given distance d_{MX}, the larger α_{X} is, the stronger is the distorsion; on the other hand, for a given value of α_X, the larger d_{MX}, the smaller is the distorsion. A polarizability α is equivalent to a volume, and hence $\alpha^{1/3}$ to a length.
– The second term is the most natural coefficient to account for the vanishing of the electronic charge distorsion when the halogen is at the center of the pyramid.

4.3 Bulk and linear compressibilities

In the case of the matlockite structure, the polyhedra bonding imply a very simple mechanism of volume compression: the mean distance between two ions is only reduced because of the bond shortening: there is no polyhedra tilting. Therefore, we define the bulk crystal as a multi-layer structure ...-MF_2-MX_2-... with the sheets perpendicular to the C_4 axis.

The linear compressibilities of the crystal, $\chi_{\perp(\parallel)} = 1/B_{a(c)}$ along the direction perpendicular (parallel) to the C_4 axis, are deduced from the knowledge of the polyhedra compressibilities using the simple elasticity arguments:

$$\frac{1}{\chi_\perp} = \sum_r \frac{q_r}{\chi_\perp^r} \quad \text{(layers bonded by “springs in parallel”)} \quad (11)$$

$$\chi_\parallel = \sum_r q_r \chi_\parallel^r \quad \text{(layers connected by “springs in series”)} \quad (12)$$

where q_r is the volumic fraction of polyhedra of type r in the total volume with $r :=$ pyr (pyramids M_{4+1}-X) or $r :=$ tetra (tetrahedra M_4-F).

Let n_r be the number of polyhedra of type r per unit cell and V_r its volume:

$$q_r = \frac{n_r V_r}{\sum_r n_r V_r}\cdot \quad (13)$$

For the matlockite compounds:

$$n_{\text{tetra}} = n_{\text{pyr}} = 2$$
$$V_{\text{tetra}} = (1/3)a^2cu'$$
$$\text{and } V_{\text{pyr}} = (1/3)a^2c(1-2u')$$

where a and c are the lattice constants and u' is the coordinate corresponding to the position of the metal in the unit cell.

Therefore:

$$q_{\text{tetra}} = \frac{n_{\text{tetra}}V_{\text{tetra}}}{n_{\text{tetra}}V_{\text{tetra}} + n_{\text{pyr}}V_{\text{pyr}}} = \frac{u'}{1-u'} \quad (14)$$

$$q_{\text{pyr}} = \frac{n_{\text{pyr}}V_{\text{pyr}}}{n_{\text{tetra}}V_{\text{tetra}} + n_{\text{pyr}}V_{\text{pyr}}} = 1 - q_{\text{tetra}} = \frac{1-2u'}{1-u'}\,. \quad (15)$$

The linear crystal compressibilities are then deduced from (11, 12):

$$\frac{1}{\chi_\perp} = \frac{q_{\text{pyr}}}{\chi_\perp^{\text{pyr}}} + \frac{q_{\text{tetra}}}{\chi_i^{\text{tetra}}} \quad (16)$$

$$\chi_\parallel = q_{\text{pyr}}\chi_\parallel^{\text{pyr}} + q_{\text{tetra}}\chi_i^{\text{tetra}} \quad (17)$$

From this, the volume compressibilities $\chi = 2\chi_\perp + \chi_\parallel (\chi = 1/B_0)$ are calculated and given in Table 2 with the experimental values for comparison.

4.4 Correlation between polyhedra and macroscopic crystal behaviour under high pressure

The compressibility perpendicular to the layers appears to be controlled by the weak M″X bonds. As a consequence, the observed contrast in linear compressibilities within the pyramid $M_{4+1}X$ may strongly influence the bulk properties of matlockite. The smaller compression of the (a) axis as compared with that of (c) is due to the relative incompressibility of the tetrahedra and of the pyramids in the direction parallel to the layers. On the other hand, the asymmetric coordination of X inside the pyramids increases the compressibility of the (c) axis. Under pressure, the X position inside the pyramid is expected to become more regular, leading, obviously, to a more tridimensional crystal.

5 Experimental

Starting from high purity materials, single crystals of MFX were grown by slowly cooling a molten mixture of carefully dehydrated MX_2 and MF_2 following the chemical reaction: $MX_2 + MF_2 \rightarrow 2MFX$ [11].

The high pressure experiments were performed using a conventional membrane diamond anvils cell [12]. The culet of the diamond anvils was 500 μm in diameter. The stainless steel gaskets were preindented to a thickness of 50 μm and drilled to a diameter of 150 μm. A fine powder of sample, made in a mortar, was loaded into the gasket hole with silicone oil as pressure transmitting medium. To measure the *in situ* pressure, the fluorescence of a ruby chip [13] placed into the gasket hole was systematically recorded before and after each experiment.

5.1 X-ray diffraction on SrFBr and PbFBr

The high pressure powder X-ray diffraction measurements were made in the energy dispersive mode at the DW11 station on the wiggler line of the DCI storage ring of the LURE (Orsay-France). After an energy calibration of the detector, the 2θ angle was determined by collecting a diffraction pattern of a copper sample placed between the diamonds. The polychromatic X-ray beam was collimated down to a 50×50 μm^2 spot centered on the gasket hole. Because of the high scattering power of the samples, exposure times between 20 and 30 min were sufficient to collect diffraction patterns with suitable peak-to-background intensity ratios.

The peak positions were determined by a Gaussian fitting of the diffracted lines. For all the compounds, 8 intense diffracted lines were selected up to the maximum pressure achieved and used in the refinement (Fig. 2). The unit-cell parameters a and c of SrFBr and PbFBr and the volume $V = a^2c$ were calculated with the least-square refinement program DICVOL [14]

In a previous X-ray diffraction study [7], a special effort has been made to increase the accuracy of the experimental measurements and allowed to describe precisely the effect of the pressure transmitting medium on the compression of layered compounds. Briefly, a strong variation of the diffraction lines width above 10 GPa has been reported when silicone oil is used as a pressure transmitting medium. This effect, commonly observed in high pressure experiments [15], may be ascribed to the glass transition of the pressure medium and is of course suspected to disturb the intrinsic behaviour of crystals under pressure. On the other hand, the lattice parameters obtained below 10 GPa with various pressure transmitting media are in good agreement, which gives confidence in low pressure measurements even when silicone oil is used. Moreover, and surprisingly, we noted that for matlockite compounds, the shifts of the lattice parameters due to the non-hydrostatic property of silicone oil seem to complement each other in order to give the value of the bulk modulus B_0 and its pressure derivative B' obtained by ultrasonic technique or by X-ray diffraction with argon as a pressure transmitting medium. Further experimental details are given in [7].

The pressure variation of the unit-cell parameters a, c and the cell volume V of SrFBr and PbFBr are given in Figures 3a and 3b respectively. Because of the previous explanations, the lattice parameters results above 10 GPa have to be considered cautiously. The isothermal

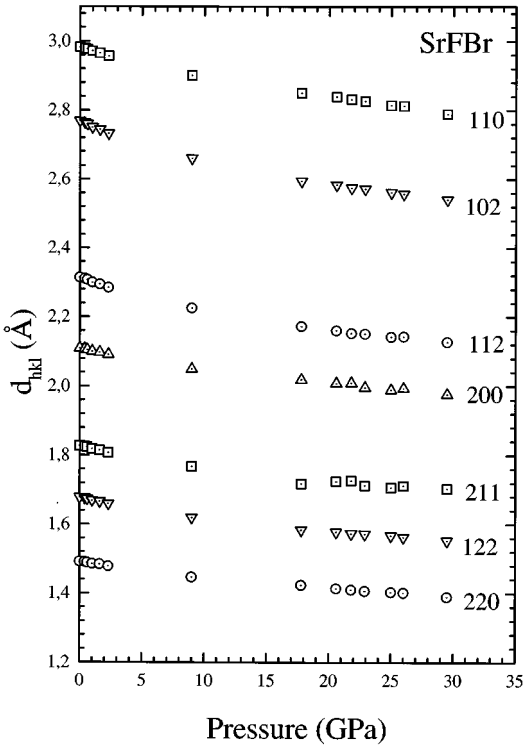

(a)

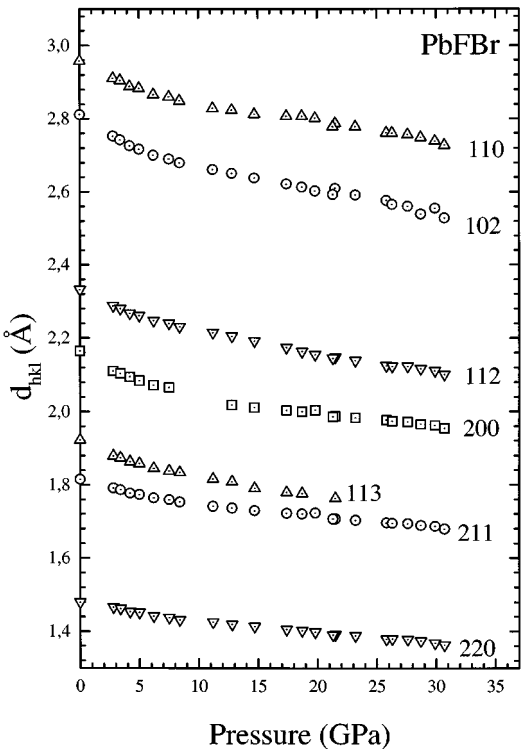

(b)

Fig. 2. Lattice spacings d_{hkl} as a function of pressure for (a) SrFBr and (b) PbFBr.

volume data points are fitted with a Murnaghan equation of state [16]:

$$\frac{V}{V_0} = \left(1 + \frac{B'}{B_0}P\right)^{-\frac{1}{B'}} \tag{18}$$

where V_0 is the cell-volume at ambient conditions. The result of the best fit is plotted in Figure 3. This fit leads to $B_0 = 51(10)$ GPa and $B' = 6(2)$ for SrFBr, and $B_0 = 43(15)$ GPa and $B' = 6(3)$ for PbFBr. This is consistent with data previously calculated by scaling factors, $B_0 = 47.8$ GPa for SrFBr, and $B_0 = 47.4$ GPa for PbFBr [17]. Moreover, a coupled Brillouin scattering/ultrasonic study [4] on SrFBr led to $B_0 = 52(6)$ GPa, in good agreement with the present diffraction data.

Because of the important deviatoric stresses above 10 GPa, only data below this pressure were considered to deduce the linear moduli from a fit with a Murnaghan equation of state, giving $B_a = 180(35)$ GPa, $B_c = 117(25)$ GPa, $B'_a = 13(7)$ and $B'_c = 14(6)$ GPa for SrFBr, and $B_a = 165(40)$ GPa, $B_c = 85(20)$ GPa, $B'_a = 20(10)$ and $B'_c = 15(8)$ GPa for PbFBr.

The complete results of this study are summarized in Table 3, together with those obtained by different experimental techniques or by a scaling factor calculation [17].

5.2 X-ray absorption spectroscopy on SrFCl and SrFBr

X-ray Absorption Spectroscopy (XAS) measurements up to about 20 GPa were performed on the D11 dispersive beamline of the LURE at strontium K edge using silicone oil as pressure transmitting medium. Bragg reflection peaks from the monocrystalline diamond anvils pollute the absorption spectra. For these experiments, a small energy range was available (150–200 eV) above the absorption edge. The Extended X-ray Absorption Fine Structure (EXAFS) signals were analyzed (with procedures previously described in Ref. [18]) by using CDXAS software [19]. The pressure dependence of the Sr-F distances in SrFCl and SrFBr is shown in Figure 4. To increase the quality of the absorption spectra, the thickness of powder loaded in the gasket hole of the diamond anvil cell has to be of the order of 30 μm, in opposition with the experimental arrangement required to observe the intrinsic layered structure behaviour without grains-grains effects. As a consequence, the results obtained above 10 GPa (deviatoric stresses due to silicone oil) are not considered as reliable. Again, we used a Murnaghan equation of state [16] to fit the experimental data in the [0–10 GPa] pressure range. Approximately, the same bond modulus was obtained for the two compounds: $B_0^{\mathrm{bond}} = 220(80)$ GPa (with a pressure derivative set to 12). To compare B_0^{bond} with the bulk modulus, it has to be divided by 3. The large difference of $(1/3)B_0^{\mathrm{bond}}$ (73 GPa) with the bulk modulus B_0 (54 GPa for SrFCl [5] and 53 GPa for SrFBr) shows that the Sr-F bonds take part only weakly to the whole compression of the structure in this pressure range, in good agreement with the assumption that the weak forces of the MFX

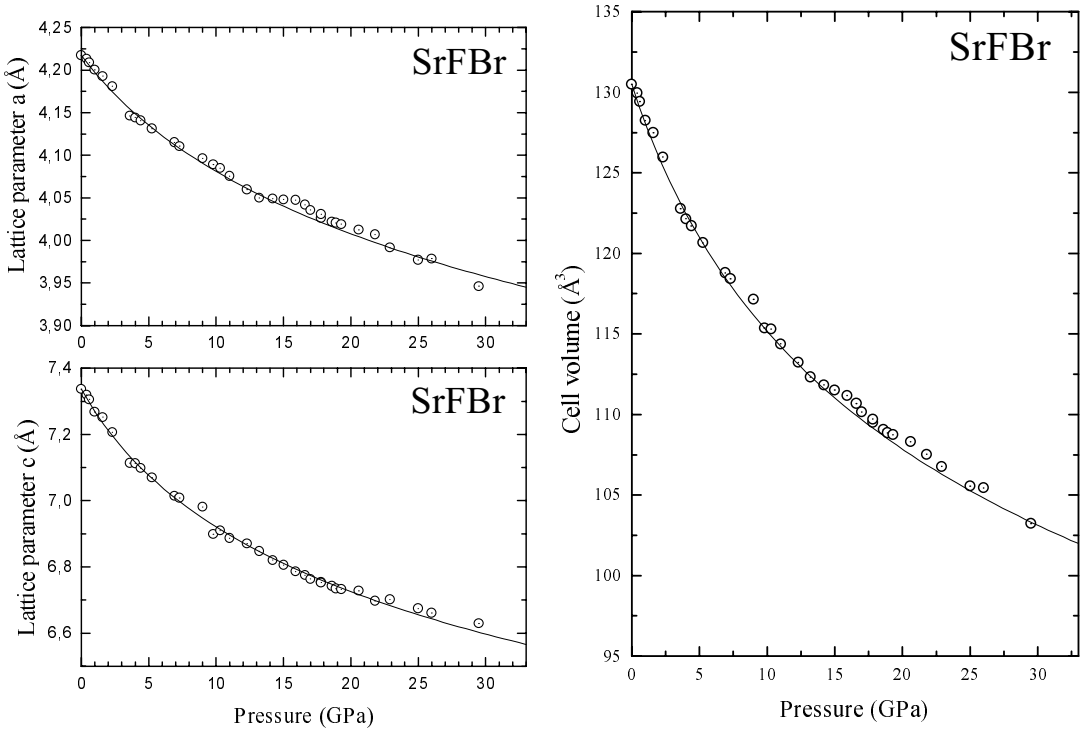

(a)

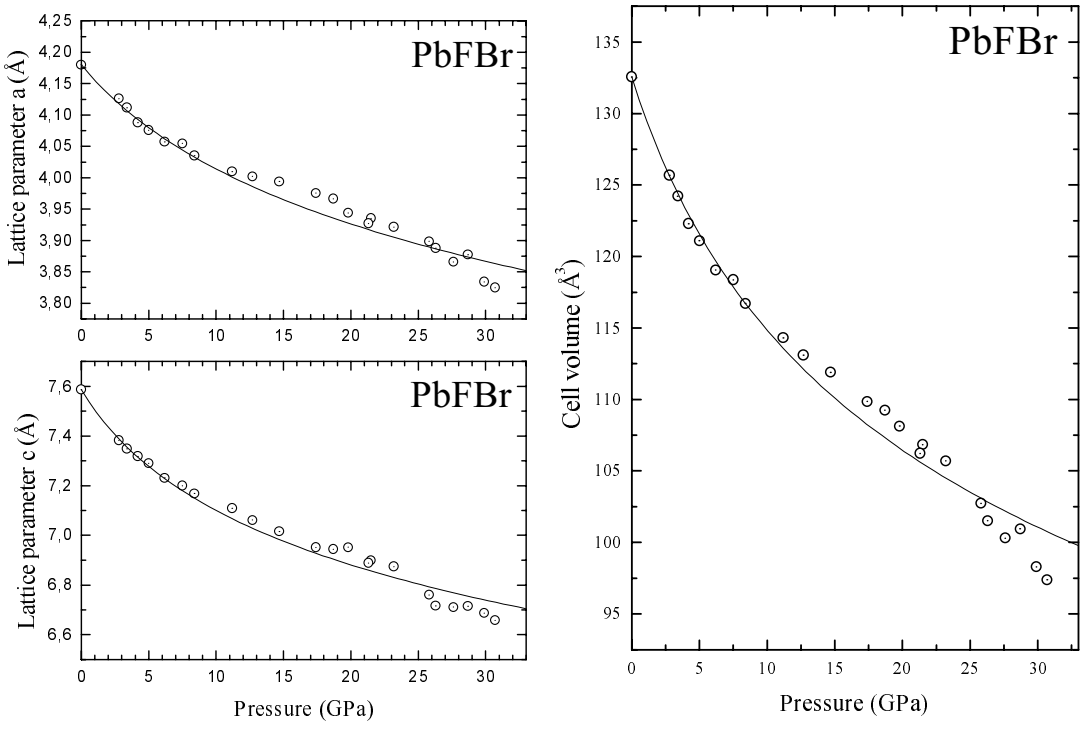

(b)

Fig. 3. Room-temperature axial and volumic compressions for SrFBr (a) and PbFBr (b) as a function of pressure. The solid curves represent the Murnaghan equation of state best fit.

Table 3. Equation of state parameters of BaFX (X=Cl, Br, I) and MFBr (M=Sr, Pb). The calculated errors include both volume and pressure measurement uncertainties.

Authors	B_a(GPa)	B'_a	B_c(GPa)	B'_c	B_0(GPa)	B'
			SrFBr			
This work[(a)]	180(35)	13(7)	117(25)	14(6)	51(10)	6(2)
Decremps[(b)] *et al.* [7]	190(30)	–	115(15)	–	52(6)	–
Sieskind[(c)] *et al.* [17]	146	–	138	–	47.8	–
			PbFBr			
This work[(a)]	165(40)	20(10)	85(20)	15(8)	43(15)	6(3)
Sieskind[(e)] *et al.* [17]	145	–	137	–	47.4	–

(a): Energy dispersive X-ray diffraction experiments on powder. (b): Ultrasonics and/or Brillouin scattering experiments. (c): Scaling factors (deduced from the shell model formulae and from the physical properties of the fluorite MF_2).

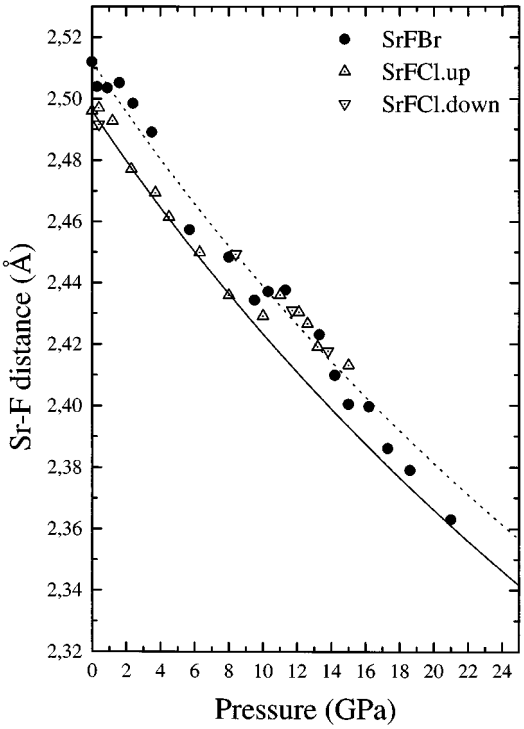

Fig. 4. Pressure dependence of the Sr-F distances in SrFCl (open triangles up (down): increasing (decreasing) pressure) and in SrFBr (full circles: increasing pressure). Lines: Murnaghan equation of state best fit. From 0 to 10 GPa, the distance measurement accuracy is about 0.01 Å, and around 0.02 Å above. (Solid: SrFCl, dashed: SrFBr)

layered compounds are localized in the $M_{4+1}X$ pyramid (between M″ and X more precisely).

As already observed in Section 4.1, the M4F tetrahedra are regular in the matlockites, with the fluorine equidistant from the cations, at the distance d_{MF}, and hence:

$$\chi_i^{\mathrm{XAS}}(\mathrm{tetra}) = \frac{1}{B_0^{\mathrm{bond}}} \qquad (19)$$

That gives for the two compounds a value of the tetrahedra isotropic linear compressibility $\chi_i^{XAS}(\mathrm{tetra}) = (4.5 \pm 0.8) \times 10^{-3}$ GPa^{-1} of in a relatively good agreement with the estimation obtained from the polyhedral method (see also Tab. 2): $\chi_i(\mathrm{tetra}) = 3.88 \times 10^{-3}$ GPa^{-1} for SrFCl and $\chi_i(\mathrm{tetra}) = 3.96 \times 10^{-3}$GPa^{-1} for SrFBr.

6 Discussion

The comparison between the volumic compressibility χ(tetra) of the M_4F tetrahedra calculated with the polyhedral method and those experimentally determined by EXAFS give confidence in the semi-empirical relation (2). The value of χ(tetra) estimated for the other compounds of the matlockite family is approximately 4×10^{-3} GPa^{-1}, *i.e.* more or less independent of the nature of the metal. This confirm the basis of the model, which stated that the anisotropy of these crystals is only dependent on the nature of the X halogen.

The model is also successful in estimating the volume compressibility of these crystals, with calculated values within 10% of the experimental ones.

On the other hand, the linear compressibilities are not so accurately reproduced, with discrepancies of about 20%. Nevertheless, the good agreement observed on the structural anisotropy ($\chi_\perp/\chi_\parallel$) of these compounds shows that it is possible to apply this model to estimate the layer character of many other ionic layered crystals (*e.g.* MX_2 as PbI_2 or CdX_2).

Unfortunately, experimental data on PbFI have not yet been obtained, but the calculation on PbFI is expected to give unreasonable results and, from this point of view, is a good example of the restrictive applicability of the present model. The polyhedral representation offers a simple way to describe complex crystal structures by reducing the atomic arrangement to a linkage of elementary geometric forms. This imply in particular a complete independence of these polyhedra: the second-nearest neighbour interactions are neglected. In the special case of PbFI, the difference between the first and second-nearest neighbour shells of the iodine is less than 10%, which does not fulfill the hypothesis of the model.

The prediction of macroscopic compressibilities is also dependent on the way the polyhedra are bonded: the matlockite structure, in which polyhedra share faces, is

a good example of a simple procedure to estimate accurately the bulk modulus from the knowledge of the polyhedra compressibilities. For some other crystals, linkages are more complex, and the procedure used to calculate the macroscopic compressibilities from the properties of the polyhedra has to take into account the polyhedral tilting.

7 Conclusion

A model, based on the polyhedral view of the crystal structure developed by Hazen *et al.* [1], is proposed to calculate the macroscopic compressibilities of layered crystals. In order to validate this model, an experimental investigation of the compressibilities of compounds belonging to the layered matlockite family has been undertaken. The local compressibility of the Sr-F bonding in SrFCl and SrFBr and the bulk moduli of SrFBr and PbFBr have been determined by EXAFS and diffraction experiments respectively. The polyhedral method, used in the matlockite, yields accurate results and is expected to be also valid for many other ionic layered crystals.

The authors gratefully acknowledge Michel Gauthier for his helpful comments.

References

1. R.M. Hazen, L.W. Finger, *Comparative Crystal Chemistry* (Wiley, New York, 1982).
2. O.L. Anderson, J.E. Nafe, J. Geophys. Res. **16**, 3951 (1986).
3. F. Decremps, M. Fischer, A. Polian, M. Sieskind, Eur. Phys. J. B **5**, 7 (1998).
4. F. Decremps, M. Fischer, A. Polian, M. Sieskind, High Temp. High Press. **30**, 235 (1998).
5. M. Fischer, A. Polian, M. Sieskind, J. Phys.-Cond. **6**, 10407 (1994).
6. Y.R. Shen, U. Englisch, L. Chudinovskikh, F. Porsch, R. Haberkorn, H.P. Beck, W.B Holzapfel, J. Phys.-Cond. **6**, 3197 (1994).
7. F. Decremps, M. Fischer, A. Polian, J.P. Itié, M. Sieskind, Phys. Rev. B **59**, 4011 (1999).
8. F. Hulliger, *Structural Chemistry of layer-type phases* (Reidel publishing, Dordrecht-Holland, 1975), p. 258.
9. M. Sieskind, J. Morel (to be published).
10. J.R. Tessman, A.H. Kahn, Phys. Rev. **92**, 890 (1953).
11. M. Sieskind, M. Ayadi, G. Zachmann, Phys. Status Sol. (b) **136**, 489 (1986).
12. R. Letoullec, J.P. Pinceaux, P. Loubeyre, High Pressure Res. **1**, 77 (1988).
13. J.D. Barnett, S. Block, G.J. Piermarini, Rev. Sci. Instrum. **44**, 1 (1973).
14. A. Boultif, D. Loüer, J. Appl. Cryst. **24**, 987 (1991).
15. J.C. Chervin, B. Canny, J.M. Besson, Ph. Pruzan, Rev. Sci. Instrum. **66**, 2595 (1995).
16. F. Birch, J. Geophys. Res. **57**, 227 (1952).
17. M. Sieskind, A. Polian, M. Fischer, F. Decremps, J. Phys. Chem. Solids **59**, 75 (1998).
18. M. Fischer, B. Bonello, J.P. Itié, A. Polian, E. Dartyge, A. Fontaine, H. Tolentino, Phys. Rev. B **42**, 8494 (1990).
19. A. San Miguel, Physica B **208-209**, 177 (1995).